remote sensing

MDPI

Article

Multitemporal–Multispectral UAS Surveys for Archaeological Research: The Case Study of San Vincenzo Al Volturno (Molise, Italy)

Nicodemo Abate [1,*], Alessia Frisetti [2], Federico Marazzi [2], Nicola Masini [3] and Rosa Lasaponara [1]

[1] Istituto di Metodologie per l'Analisi Ambientale (IMAA), National Research Council (CNR), C.da Santa Loja, 85050 Tito Scalo, Italy; rosa.lasaponara@imaa.cnr.it
[2] Department of Humanities, Univerity of Naples Suor Orsola Benincasa, Corso Vittorio Emanuele, 292, 80132 Napoli, Italy; alessia.frisetti@docenti.unisob.na.it (A.F.); federico.marazzi@docenti.unisob.na.it (F.M.)
[3] Istituto di Scienze del Patrimonio Culturale (ISPC), National Research Council (CNR), C.da Santa Loja, 85050 Tito Scalo, Italy; nicola.masini@cnr.it
* Correspondence: nicodemo.abate@imaa.cnr.it; Tel.: +39-33-3336-6056

Abstract: Unmanned aerial vehicles are currently the most used solution for cultural heritage in the field of close range and low altitude acquisitions. This work shows data acquired by multitemporal and multispectral aerial surveys in the archaeological site of San Vincenzo al Volturno (Molise, Italy). The site is one of the most important medieval archaeological sites in the world. It is a monastic settlement that was particularly rich during the early Middle Ages, and is famous for its two full-frescoed crypts which represent a milestone in the history of medieval art. Thanks to the use of multispectral aerial photography at different times of the year, an area not accessible to archaeological excavation has been investigated. To avoid redundancy of information and reduce the number of data to be analysed, a method based on spectral and radiometric enhancement techniques combined with a selective principal component analysis was used for the identification of useful information. The combination of already published archaeological data and new remote sensing discoveries, has allowed to better define the situation of the abbey during the building phases of the 8th/9th century and 11th century, confirming and adding new data to the assumptions made by archaeologists.

Keywords: medieval archaeology; remote sensing; drones; multispectral analysis; multitemporal analysis; San Vincenzo al Volturno; Principal Component Analysis

Citation: Abate, N.; Frisetti, A.; Marazzi, F.; Masini, N.; Lasaponara, R. Multitemporal–Multispectral UAS Surveys for Archaeological Research: The Case Study of San Vincenzo Al Volturno (Molise, Italy). *Remote Sens.* **2021**, *13*, 2719. https://doi.org/10.3390/rs13142719

Academic Editors: Devrim Akca and Taejung Kim

Received: 7 June 2021
Accepted: 8 July 2021
Published: 10 July 2021

1. Introduction

In the context of close range acquisitions at relatively low altitudes, UASs (unmanned aerial systems) are currently one of the most used solutions for cultural heritage (CH). They have become a key-tool in the field of remote sensing for CH. In fact, the development of high-performance and low-cost UASs has allowed to not use planes and helicopters, common tools in aerial archaeology, for minor acquisitions [1–4]. The exponential increase in activities related to the use of UASs in archaeology has significantly increased the number of publications in this field [5].

In particular, UASs are used for activities such as (i) three-dimensional survey and documentation of archaeological sites and excavations, (ii) documentation of monuments, and (iii) large-scale survey for landscape archaeology. A considerable advantage is the possibility to fly over any area and, with the necessary precautions, to reach places not accessible with other instruments, terrestrial or airborne. Another strong point is to be able to adapt UASs with different payloads according to the need and purpose of the acquisition. Payload is the load, in terms of weight, that can be achieved by a UAS. Consumer drones support a light-weight load (max 800 g) but often it is enough to adapt several sensors. Most used sensors in archaeological field are:

(i) RGB cameras [6–13];
(ii) Multispectral/hyperspectral cameras and thermal imaging cameras [14–21];
(iii) LiDAR (Light Detection And Ranging) [22–26].

RGB cameras are certainly the most used sensors and, usually, are already supplied with the UAS. RGB sensors allow to capture images in visible wavelengths (430–700 nm) that can be processed with three-dimensional photogrammetry or SFM (structure from motion) software. The accuracy of the survey is closely linked to several factors, such as (i) calibration of the cameras, (ii) use of photogrammetric markers and ground control points (GCPs), (iii) use of external equipment (e.g., Real Time Kinematic, total stations, GPS, etc.). Software can return several outputs, such as point cloud, three-dimensional model, textured model, etc. [27–30]. In addition to the RGB sensor, a payload that can be adapted is a multispectral camera to analyse wavelengths beyond the visible spectrum. The analysis of multispectral images allows to understand the relationship that exists between the presence of buried archaeological elements and the vegetation present on the surface [31–33].

The identification of archaeological features in images is facilitated by the change in reflectance of vegetation in certain areas. This change generates a clearly visible contrast in multispectral images between the archaeological features and their surroundings, particularly in the Red, Green, Near Infrared and Red-edge channels [34–39].

The same contrast is also accentuated within calculated images (indices), the result of the mathematical combination of channels, useful for assessing the health of the vegetation, the level of humidity and the production of chlorophyll [40,41]. Depressions, cavities and structures in subsoil influence local phenology, which is more or less vigorous depending on the type of presence. Archaeological features are usually more evident during the early stages of growth, when it is strongly influenced by soil moisture [42–45].

The purpose of this paper is to show the results obtained from the analysis of multispectral–multitemporal data acquired during a campaign of four acquisitions by UAS, in the archaeological site of San Vincenzo al Volturno (Molise, Italy). The use of remote sensing (RS) techniques by drone has allowed to investigate an area outside the current area of the archaeological site, allowing to make assumptions with non-invasive techniques about the presence of buried remains in an area that cannot be investigated, to date, with the normal techniques of archaeological excavation.

2. Materials and Methods

2.1. Study Area

The area of interest (AOI) was chosen due to the hypothesis of buried buildings, located south of the archaeological site (Figure 1). The place is perfect to test remote sensing (RS) techniques such as UASs: (i) it is far from private buildings and main streets or rails; (ii) it is in a low-traffic area; (iii) it is in an open private property, bordering to the public properties; (iv) non-invasive techniques are allowed without restrictions.

The archaeological site of San Vincenzo al Volturno is one of the most important sites in Europe for the early medieval period. According to ancient sources, the monastery was founded at the beginning of the 8th century by three noblemen from Benevento (Campania, Italy) who sought to embrace a monastic life [46,47].

They settled among previously existing late Roman buildings, near the river Volturno. During the 9th century, the monastery reached its zenith thanks to support received by Carolingian emperors. In this period the monastic complex grew to considerable size, inhabited by a community of several hundred monks. Information about the number of monks in the monastery is given by the size of the buildings (e.g., refectory). The monastic refectory, dating to the 9th century, is a rectangular building 31 m long and 11 m wide. The building was constructed with the floor slightly sloping towards the river. Along the walls and among the central columns a bench was built to allow some 300 monks to sit down and have their meals. It ran a landed patrimony spanning several areas of southern Italy (Figure 2a).

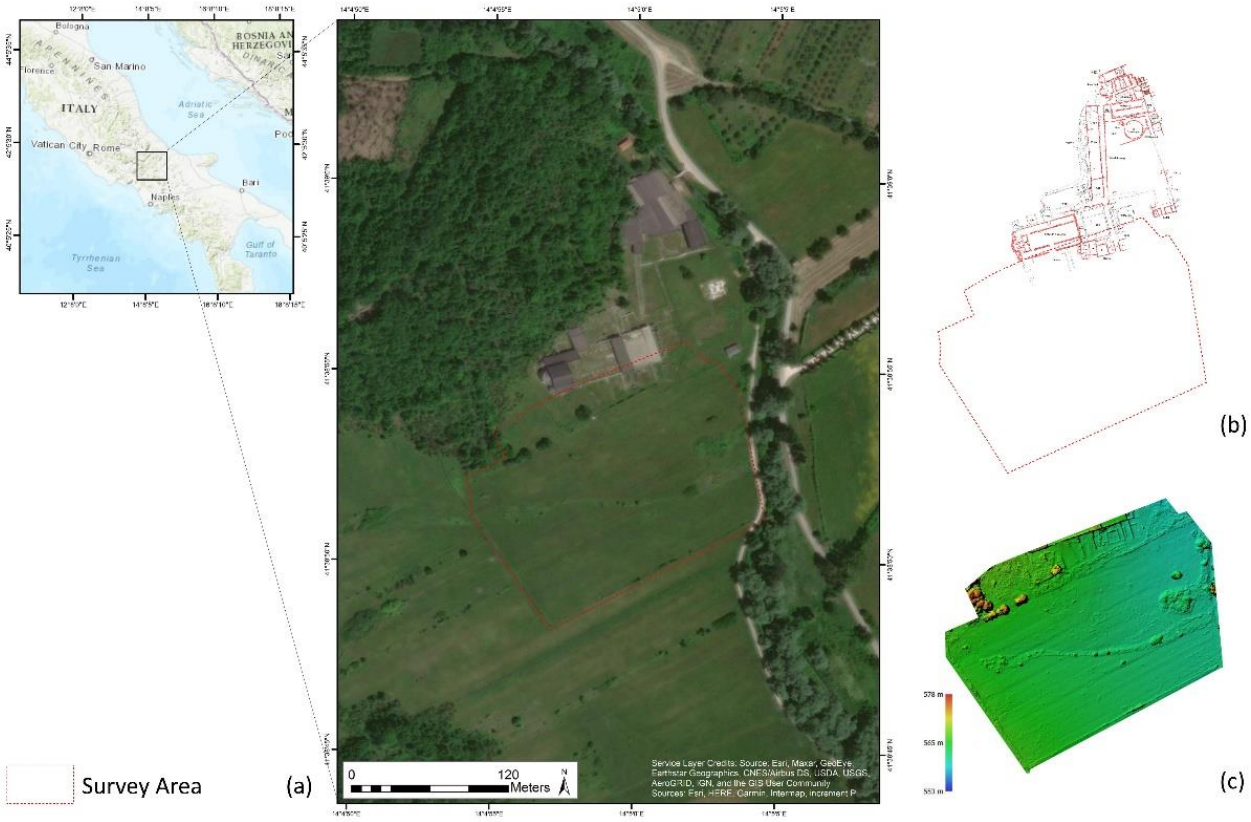

Figure 1. Archaeological area of San Vincenzo al Volturno (Isernia, Molise, Italy): (**a**) location of the survey area; (**b**) overlay of the survey area with the structures surveyed by archaeologists during excavations (1980–2019); (**c**) digital elevation model (DEM) obtained from the image acquired on 16 July 2019. The coordinate system used was WGS 1984 UTM Zone 33N; EPSG: 32633.

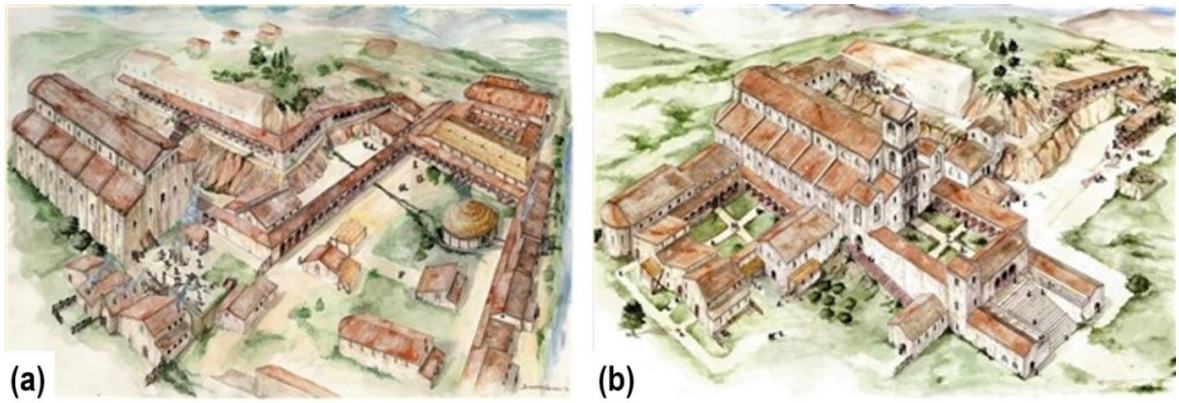

Figure 2. (**a**) Reconstructive hypothesis of the monastery during the early Middle Ages; (**b**) reconstructive hypothesis of the monastery during the late Middle Ages (drawings by S. Carracillo, both available on www.sanvincenzoalvolturno.it, accessed on 29 June 2021).

The monastic buildings of this phase (refectory, assembly room, vestibule, churches and a garden court) were grouped around an open central space and the main abbey church stood in the southwestern corner. Dating back to the 9th century are the main churches of the monastery built by the so-called builder-abbots Joshua, Talaric, and Epiphany: the main basilica (Basilica Maior) with the crypt of Joshua and the church and crypt of Epiphany. Both these buildings represent a milestone for the study of medieval art-history in the world, thanks to their architecture and frescoes. The monastery suffered a strong setback due to an earthquake (848 A.D.) and an Arab attack (881 A.D.). The settlement was destroyed

by fire during the attack and the surviving monks left the place for 30 years. After this period, monks returned in Molise and re-built part of the monastery. The monastery had another period of prosperity during the 11th century. The development of the monastery during this new phase, differed profoundly from the previous one because it acquired a well-defined planimetric scheme, typical of those centuries, although it partly reoccupied the spaces already built [48]. In the 11th century, the abbey of San Vincenzo was rebuilt following a plan largely different from that of Carolingian times. New buildings were developed around the main church and a rectangular cloister was built on its southern side (Figure 2b).

The abbey was abandoned during the 12th century and the monks established a new monastery on the opposite side of the Volturno [49,50].

The importance of the archaeological site of San Vincenzo was rediscovered during the 20th century, after the fortuitous discovery of the crypt of Epifanio by a local farmer. The archaeological excavations in the site of San Vincenzo al Volturno began in the 80s. At present, a campaign of archaeological excavations is scheduled every year between July and September, directed by Prof. F. Marazzi (Università degli Studi Suor Orsola Benincasa di Napoli).

Before the beginning of the archaeological activity, the area was dedicated to the cultivation of vines and olive trees, and later to agriculture and pasture, as the entire plain of the Volturno river; this is visible within the images acquired by the Military Geographical Institute of the Italian State (IGM) since the 1940s (Figure 3).

Analysis of historical data/maps and aerial photos is a common practice in the study of the ancient landscape and, during the last decades, has led to the discovery of archaeological sites around the world [33,51–58]. Traces of palaeo land use are still clearly visible within photos acquired during the last century by planes and high-resolution satellite platform (e.g., Google Earth or ESRI), and are identifiable during archaeological excavations, as (i) large holes due to tree removal, (ii) large accumulations of agricultural soil, (iii) archaeological material shredded and dispersed by mechanised agricultural activity [59].

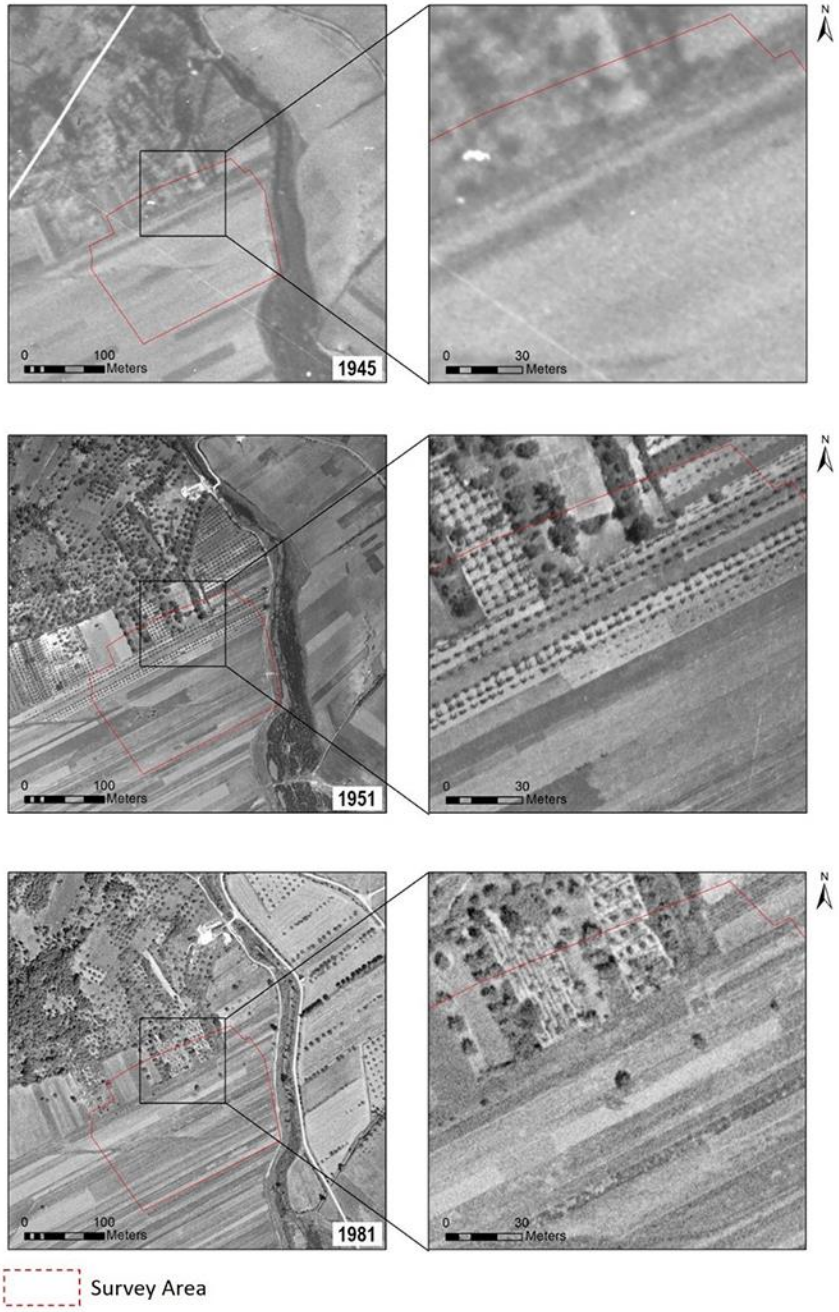

Figure 3. Aerial images acquired by Military Geographical Institute of the Italian State (IGM) during 1945, 1951, and 1981 (Fotografie Aeree dell'Istituto Geografico Militare (Autorizzazione n. 7084 datata 29/06/2021; www.igmi.org).

2.2. UAS, Camera and Acquisition Methods

The investigation in the abbey of San Vincenzo al Volturno was carried out using a Parrot Ag Disco Pro, produced by Parrot SA, Paris, France (Table 1).

It is a fixed-wing UAS, equipped with a multispectral camera (Parrot Sequoia). Parrot Sequoia is a camera with several sensors that allow to acquire images in the wavelengths of Green (550 nm), Red (660 nm), Red-Edge (735 nm), Near Infrared (790 nm), and a single RGB camera (16 mpx). In addition, the camera uses an external brightness sensor (sunshine) that collects and records real-time data on light conditions, allowing a perfect normalisation of the images (Figure 4).

Table 1. Summary of the flight and processing parameters.

flight dates	1 July, 12 August, 16 September 2019
multispectral camera	Parrot Sequoia+
reflectance panel	Parrot Sequoia reflectance panel
RGB resolution	16 mpx
multispectral resolution	2 mpx
acquired bands	Green, Red, Red-Edge, NIR
used UAS	Parrot Ag Disco Pro
useful hectares per flight	6.5 ha
flight height	50 m
flight speed	13 m/s ca.
time of day	between 10 and 12 a.m.
multispectral photos per flight	580
RGB photos per flight	145
overlap	80% (frontal and lateral)
dense cloud (high quality)	6.667.479 points
density point	98.7 points/m^2
tie point	454,576

Figure 4. Images acquired during the survey activities. The operator is working on (**a**) compass calibration and (**b**) take-off. (**a**) 1 July 2019; (**b**) 16 September 2019.

Flight operations were conducted using Pix4D capture app for IOS. The application allows to select an area of interest for the survey, and manages the flight autonomously, after setting speed, overlap between shots and flight height. The flight parameters were constant for the entire duration of the activity. During each session, the drone reached a height of 50 m above the take-off point and a cruising speed of 13 m/s (46 km/h). The overlap of the photos was constant, with a frontal and lateral overlap of 80%. The acquisition phase was carried out from July to September 2019, for a total of three flights. The area covered by the survey is 0.065 km^2/6.5 ha and it is located to the south of the abbey, outside the modern boundary of the archaeological site. The area was chosen because it is relevant for the knowledge of the development of the urban plan of the monastery to the south. However, the area is outside the archaeological site and can only be analysed by remote sensing analysis. Each flight allowed to acquire 580 images (145 for each spectral band).

2.3. Data Processing

The data processing was carried out following the flowchart shown in Figure 5.

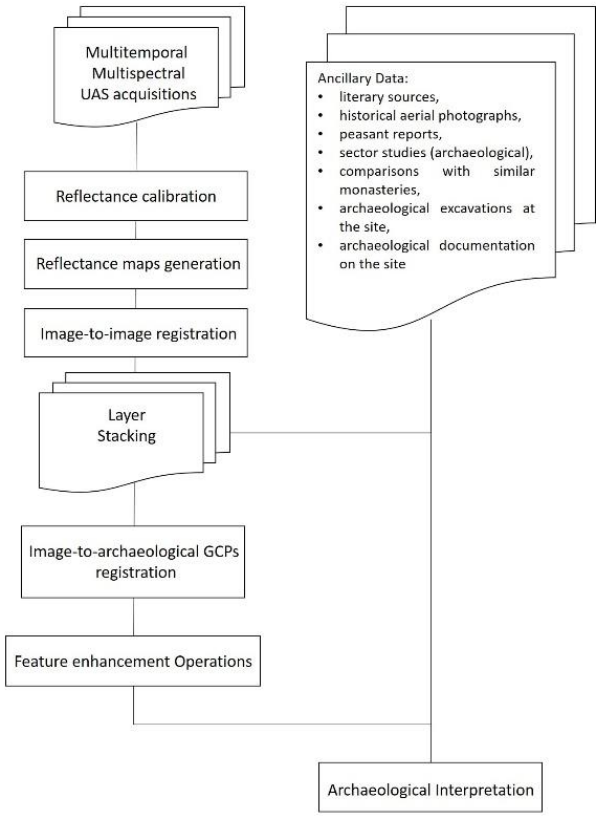

Figure 5. Flowchart.

Multispectral images were processed using different software and methodologies. Multispectral images were pre-processed using Agisoft Metashape software, useful for the creation of orthophotomosaics and reflectance maps. The acquired images were radiometrically corrected thanks to the use of a Parrot Sequoia reflectance panel. The processed multispectral orthophotomosaics had a GSD (ground sampling distance) between 4 and 5 cm/pixel. Metashape s generated orthophotomosaics of images in the channels of Red, Green, Nir, Red-edge and their respective reflectance maps, in GeoTIFF format. The photo alignment for each flight was produced in several steps: (i) creation of the point cloud (sparse and dense) using "high" as processing parameter; (ii) the alignment of the point clouds was achieved using the "align using markers" tool of the Metashape software, identifying within the photos homologous fixed points above known structures and elements (panels, modern buildings, field boundary elements) in order to have a homogeneous distribution of markers along the edges and within the survey area to create an alignment based on the source images (image-to-image); (iii) then the processed data for each flight were used to produce DEMs (digital elevation models) and orthophotomosaics; (iv) the data thus produced were exported to be processed in other software.

The produced outputs were then aligned to the archaeological evidence discovered during excavations from 1980 to 2019, using maps produced by archaeologists using co-registration tools in ArcMap, based on a GCP (ground control point) alignment process. The alignment was done taking into account the structures visible both in the archaeological surveys and in the orthophotos produced by drone in order to preserve the alignment of the features for the remote sensing analysis. In fact, the idea behind this alignment was to preserve mainly this alignment, so as to facilitate the archaeological interpretation of the features observed by drone.

The processed files were then processed in SAGA Gis software, an open source software, for the operations of (i) resampling, (ii) clipping, and then (iii) exporting with new proprieties as a layer-stack. The resampling tool was essential to be able to work with all the data at the same time, bringing the pixels of each image to the same size. Resampling is the process of determining new values of cells (pixels) in a grid (image) that result from applying some geometric transformation to an input image, referring to a reference image or a set parameter. The transformation can be of different types: (i) nearest neighbour assignment, (ii) bilinear interpolation, and (iii) cubic convolution. In this case, resampling with nearest neighbour assignment was used [60,61].

Images were then processed to improve the visualisation of features of archaeological interest as described in the following paragraphs.

2.4. Feature Enhancement Operations

Local differences in soil moisture and vegetation health are identifiable thanks to reflectance maps. In the context of archaeological research, these differences are called archaeological proxy indicators and are used by archaeologists to hypothesise the presence of buried structures on the basis of possible recognisable patterns (e.g., geometric features). These are created by the presence of buried structures or traces, or by anthropogenic actions that create discontinuities in soil permeability or positively/negatively affect vegetation growth and health [62–64].

Enhance the visibility of proxy indicators, also called crop- and soil-marks, is possible thanks to the use of several methods and is a mandatory step in remote sensing (RS) techniques applied to archaeology.

To enhance the visual interpretation of crop- and soil-marks, several enhancing techniques were applied, according to RS literature, such as (i) radiometric enhancement, (ii) spectral enhancement (indices based); (iii) transformation (principal component analysis).

2.4.1. Radiometric Enhancement

The first operation carried out on coregistred and resampled images was a radiometric enhancement applied to Nir-Red-Green composites, also called False Color Infrared (FCIR) images, and single bands. The radiometric enhancement is a simple pixel-based technique useful to enhance the presence of differences in pixel value, through changes made to the histogram of individual bands in an image, working on brightness and contrast, characteristics related to reflectance [34,65] (Figure 6).

Histogram techniques can be applied on gray-level images, single channel, images or on RGB (multichannel) images, completely changing the rendering of the final result compared to the initial one [66]. According to Lasaponara and Masini [63,64], radiometric enhancement techniques used were (i) minimum–maximum and percentage linear contrast stretch (linear technique), (ii) histogram equalisation (nonlinear techniques). Both techniques were applied with the aim to increase the contrast and improve the identification of features of archaeological interest and select them from the background (see Section 2.4.2). The linear enhancement techniques are based on contrast stretching using (i) percentage (e.g., 1%, 2%, 5%), (ii) standard deviation (e.g., ± 1 σ, ± 2 σ, ± 3 σ), or (iii) imposed values, to expand the original values into a new distribution. Software and platforms (e.g., ENVI, R, Qgis, Arcmap, Matlab, Google Earth Engine, etc.) allow through a specific function to identify the minimum and maximum values on which to scale the image [67] (Figure 7).

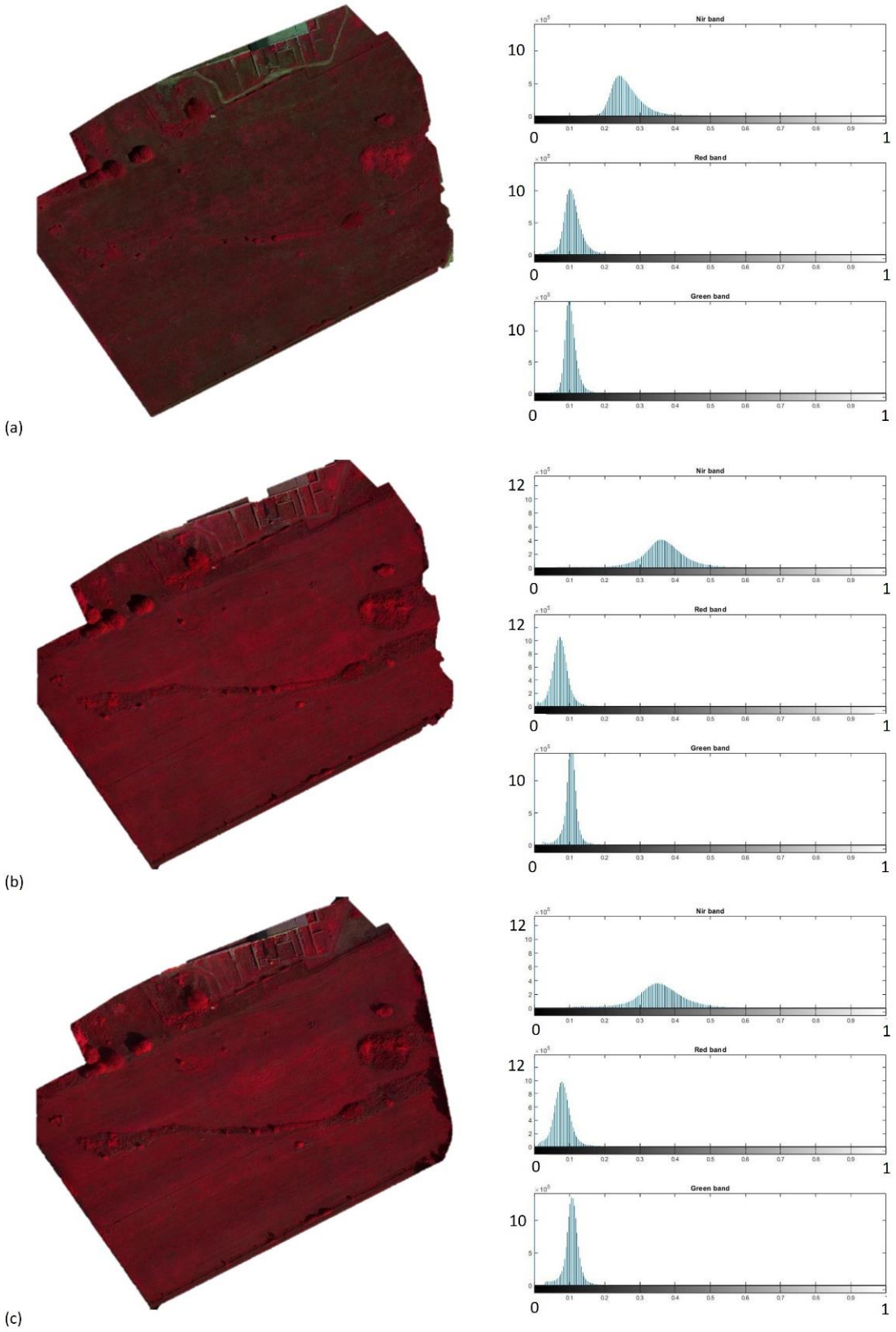

Figure 6. FCIR composite and single band histogram: (**a**) July, (**b**) August, and (**c**) September.

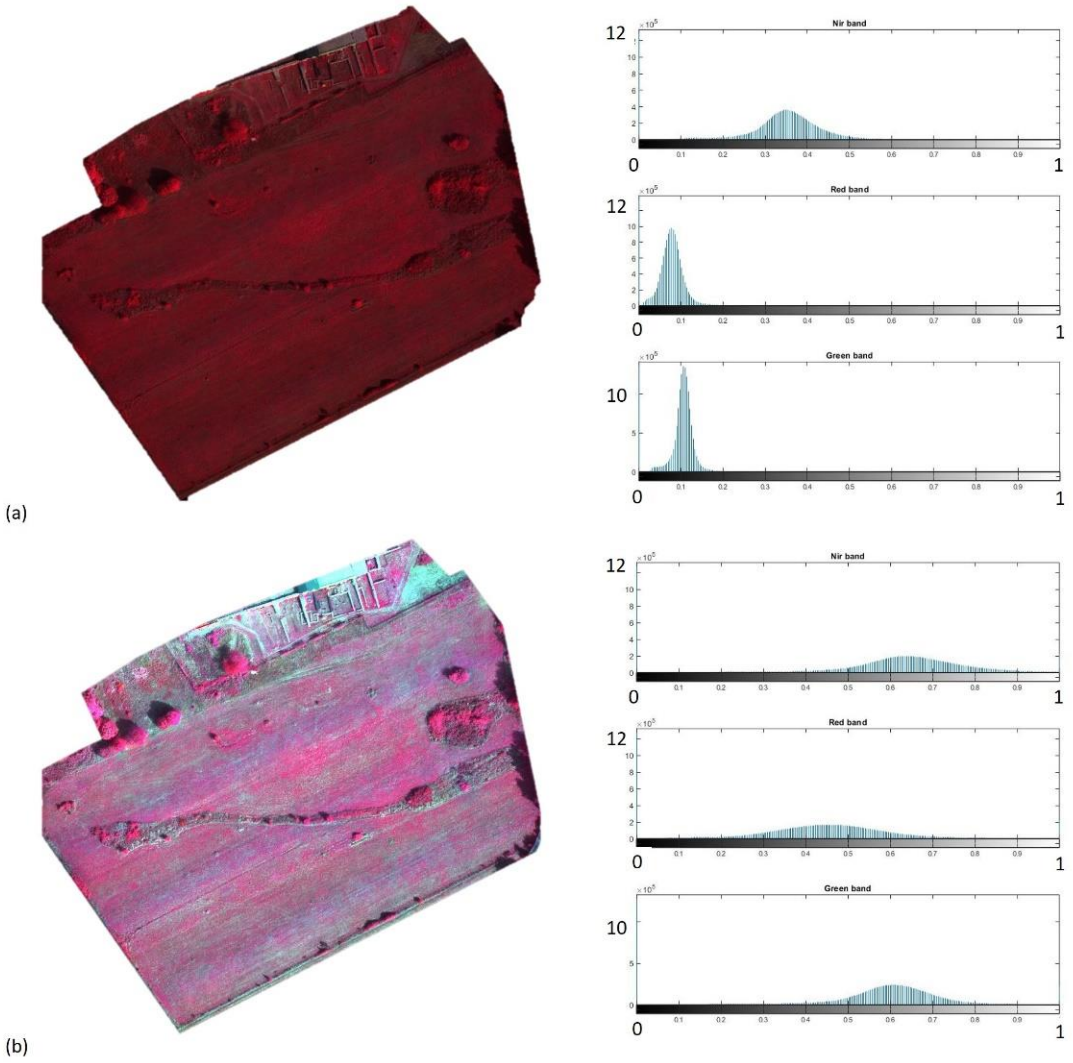

Figure 7. Example of linear enhancement techniques applied on September image: (**a**) FCIR image; (**b**) transformed FCIR image.

Histogram equalisation methods are probably the most common nonlinear contrast enhancement methods. Histogram equalisation techniques herein proposed are divided into two approaches: (i) global histogram equalisation (GHE), and (ii) adaptive histogram equalisation (AHE). In the GHE the histogram of the input image is used for the transformation, resulting in a flattened and stretched histogram; while in AHE, several local histograms are calculated and used to improve local contrasts [68,69] (Figure 8).

Radiometric improvement techniques were also applied to the results obtained from the principal component analysis process (see results and discussion).

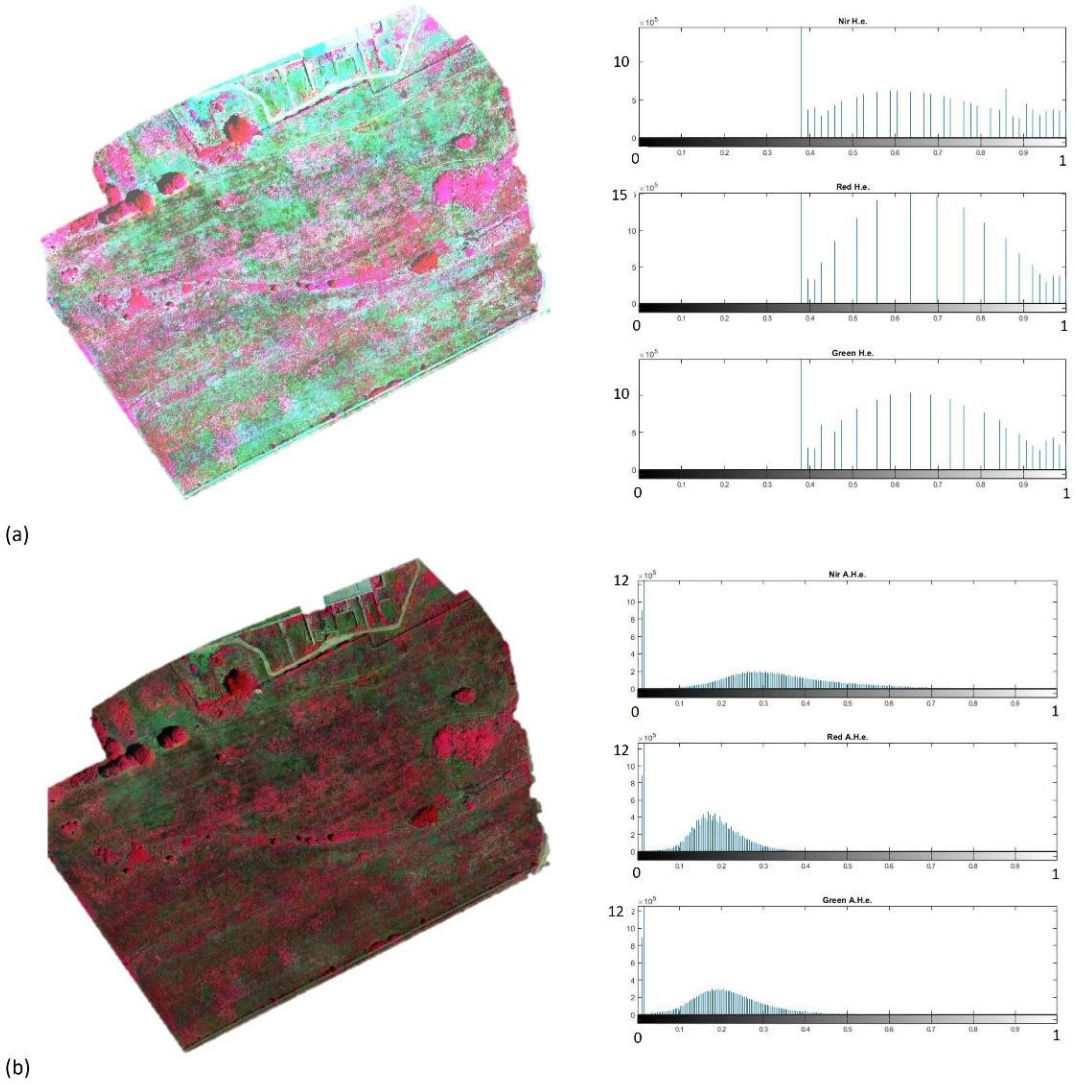

Figure 8. Example of (**a**) histogram equalisation and (**b**) adaptive histogram equalisation applied to July image.

2.4.2. Spectral Enhancement

Spectral enhancement techniques were applied to enhance the features in relation to their spectral signature, in order to identify the features of archaeological interest and therefore the presence of buried elements. The most common and simple spectral enhancement technique that can be applied in the context of RS for cultural heritage is the creation of indices [63,64].

Indices are created by performing mathematical operations using the individual bands, and their spectral characteristics, to create new images. Indices have several functions and are based on the different individual bands involved in their creation. Those considered for this type of analysis, and for archaeology in general, were (i) indices for monitoring vegetation health and chlorophyll percentage, useful to enhance differences between healthy and unhealthy vegetation, and (ii) indices useful to identify differences in soil moisture [31,38,70–72] (Figure 9).

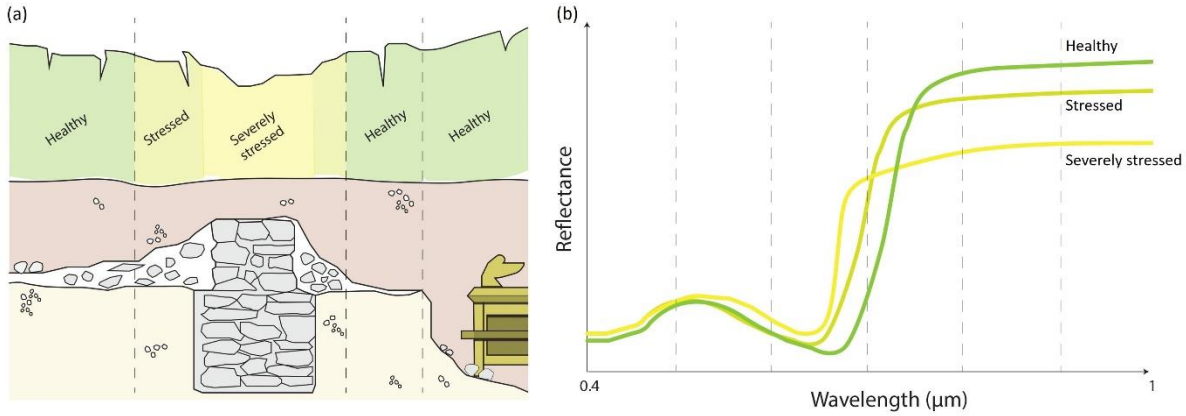

Figure 9. Example of crop-marks pattern in relation to the presence of buried remains (drawn by the authors): (**a**) illustrative diagram of the reaction of the health of the vegetation in relation to the subsoil; (**b**) illustrative diagram of the reflectance recorded in cases similar to (**a**).

Through mathematical operations between reflectance bands, several indices were obtained (Table 2).

Table 2. Calculated indices.

Index	Equation	Reference
Difference Vegetation Index (DVI)	$NIR - Red$	[73]
Green Difference Vegetation Index (GDVI)	$NIR - Green$	[74]
Green Normalised Difference Vegetation Index (GNDVI)	$\frac{(NIR-Green)}{(NIR+Green)}$	[74]
Green Ratio Vegetation Index (GRVI)	$\frac{NIR}{Green}$	[42]
Normalised Difference Vegetation Index (NDVI)	$\frac{(NIR-Red)}{(NIR+Red)}$	[75]
Optimised Soil Adjusted Vegetation Index (OSAVI)	$\frac{1.5\times(NIR-Red)}{NIR+Red+0.16}$	[42]
Modified Simple Ratio (MSR)	$\frac{\left(\frac{NIR}{Red}\right)-1}{\left(\sqrt{\frac{NIR}{Red}}\right)+1}$	[72]
Advanced Vegetation Index (AVI)	$[NIR * (1 - Red) * (NIR - Red)]^{1/3}$	[42]
Nonlinear Vegetation Index (NLI)	$\frac{NIR^2-Red}{NIR^2+Red}$	[71]

Among the most used is certainly NDVI index (Normalised Difference Vegetation Index). NDVI is an NIR-based index, useful for the study of canopy health and ranges between −1 and +1, where negative values or values close to 0 correspond to bare soil, buildings and water, while values close to 1 indicate thick and healthy vegetation, although this is closely related to phenology, vegetation type and season [76].

Other calculated indices were similar to NDVI, such as (i) GNDVI (Green Normalised Difference Vegetation Index) and (ii) GRVI (Green Ratio Vegetation Index), but more sensitive to chlorophyll concentration [73,77].

Spectral enhancement techniques are certainly one of the first steps to facilitate the interpretation of images and the recognition of potentially buried remains [34]. The difference between the features in the images, characterised by a different spectral response, was the basis for the recognition and enhancement of the features from a spectral and geometric point of view. The archaeological proxy indicators visually identified within the data were therefore marked as features of archaeological interest or point of interest (POIs) and distinguished from the immediate surroundings, where presumably there are no remains of archaeological interest. After the identification of the POIs, the spectral signature of the features of archaeological interest in all bands and indices was plotted and

spectral separability between POIs and their surrounding was calculated using M-statistic method [78] (1):

$$M = (\mu_1 - \mu_2)/(\sigma_1 + \sigma_2), \quad (1)$$

where, μ_1 is the mean value for class POIs, μ_2 is the mean value for the background and σ_1 and σ_2 are the respective standard deviation.

The M-statistic tests the separation between the histograms produced by plotting the pixel values within two classes. Good separability is achieved for M > 1 [79]. The extracted graphs were useful to identify the best performing bands and indices, over time, for the identification of features of archaeological interest (Figure 10).

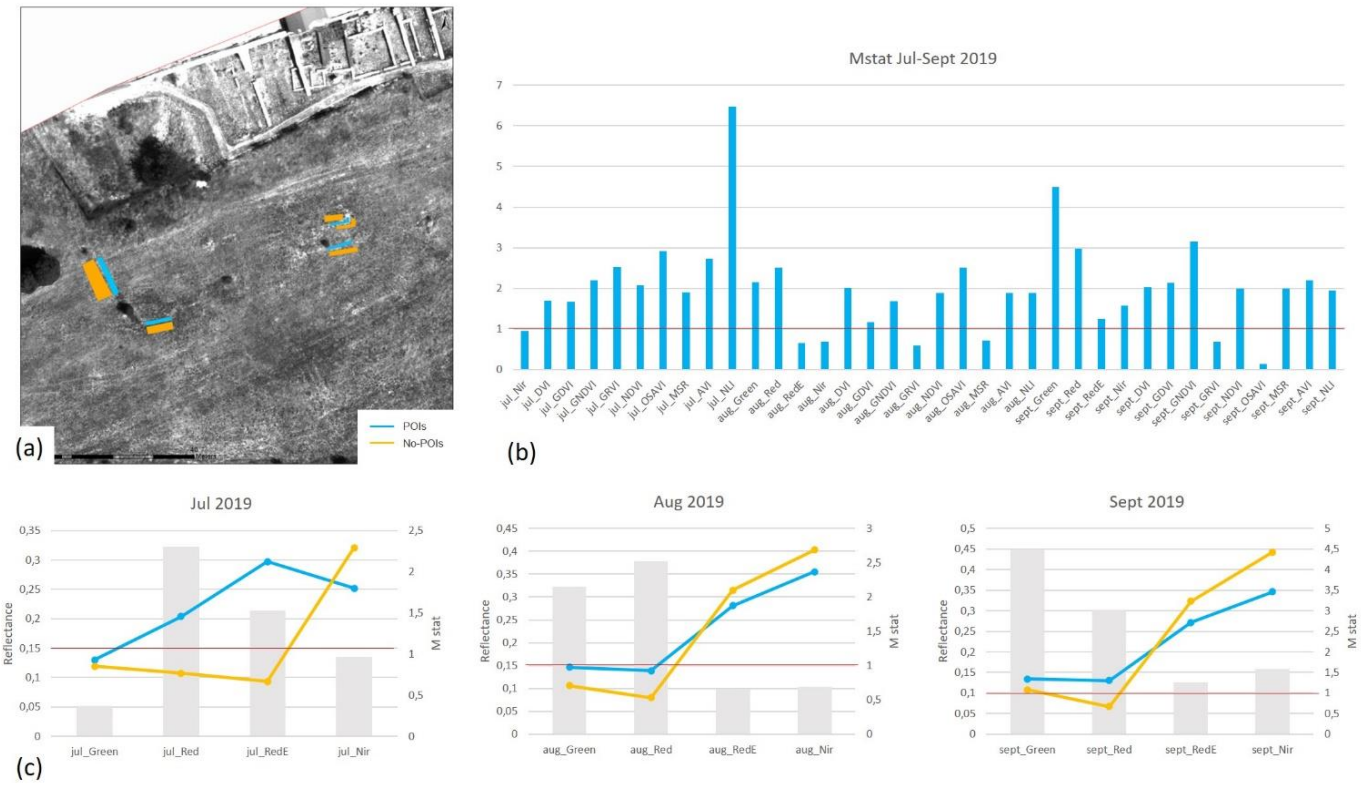

Figure 10. In the graphs, the lines represent the reflectance, referring to (**a**), while the columns represent the statistical M value: (**a**) points of interest selected for the reflectance calculation: (POIs) selection, where the presence of archaeological remains is expected, and points of no interest (No-POIs), where the presence of archaeological remains is not expected; (**b**) M-statistic of the individual bands and of the calculated indices, with reference to the threshold of value 1 used to filter the bands for the SPCA calculation; (**c**) example of the reflectance (left-vertical axis) and statistical M (right-vertical axis) for Green, Red, Red-Edge, and NIR from the July to September acquisitions, with reference to the threshold of value 1 used to filter the bands for the SPCA calculation.

The indices produced were (i) analysed individually and selected for their spectral properties (Figure 10), (ii) transformed through principal component analysis in new outputs.

2.4.3. Data Reduction

Using groups of images and indices, a PCA (principal component analysis) was performed to reduce redundancy of information, and, of course, reduce the number of inputs to be analysed for the identification of features of archaeological interest. PCA is one of the most used and oldest methods for data reduction, useful to operate with a large dataset and to reduce input dimensions "preserving as much variability as possible" [80]. The PCA is a technique of data simplification. It was already used in the past to enhance the presence of archaeological proxy indicators, for hyperspectral and multispectral images [81–84]. Its aim is to reduce the number of variables present in the most representative ones. In the case of

multispectral images, the PCA considers the images as matrices of numbers (the pixel value also defined as spectral signature). The PCA generates new images decorrelated to each other, in number equal to the input data [85,86]. PCA is a very useful tool to reduce redundancies but there are some risks such as the possibility of losing useful data (small features) by only looking at the first components [85]. PCA involves specific steps: (i) averaging the pixels of the input images, creating an image of the average, and subtracting the computed mean image from each input image; (ii) computing the covariance (or correlation) matrix over all input bands; (iii) decomposing the eigenvalue of the covariance matrix to obtain new images, called components. Overall, PCA is a linear transformation that transforms a number of correlated variables into a (smaller) number of uncorrelated variables, that still preserve much of the information present in the input data set. This allows the information to be concentrated within a few components [87,88].

For this study PCA was performed using correlation matrix method in SAGA Gis software. The process was obtained using all images with threshold M > 1: (i) individual bands per acquisition day, and (ii) produced indices [89]. This method, called selective principal component analysis (SPCA), is already known in the literature and consists of transforming only the bands or indices assessed to be most efficient in extracting useful information for archaeological research [90]. In accordance with the literature on the issue, PCs produced were not unambiguous and not all PCs were useful [91], as displayed by the RGB combination (R: 1st PC; G: 2nd PC; B: 3rd PC) in Figure 11.

Figure 11. R: 1st PC; G: 2nd PC; B: 3rd; SPCAs obtained using correlation-matrix method.

In this case, the most significant bands were autoptically selected from those generated and used for the recognition of features of possible archaeological interest, as is shown in the Figure 12 where R: 4th PC; G: 23th PC; B: 27th PC.

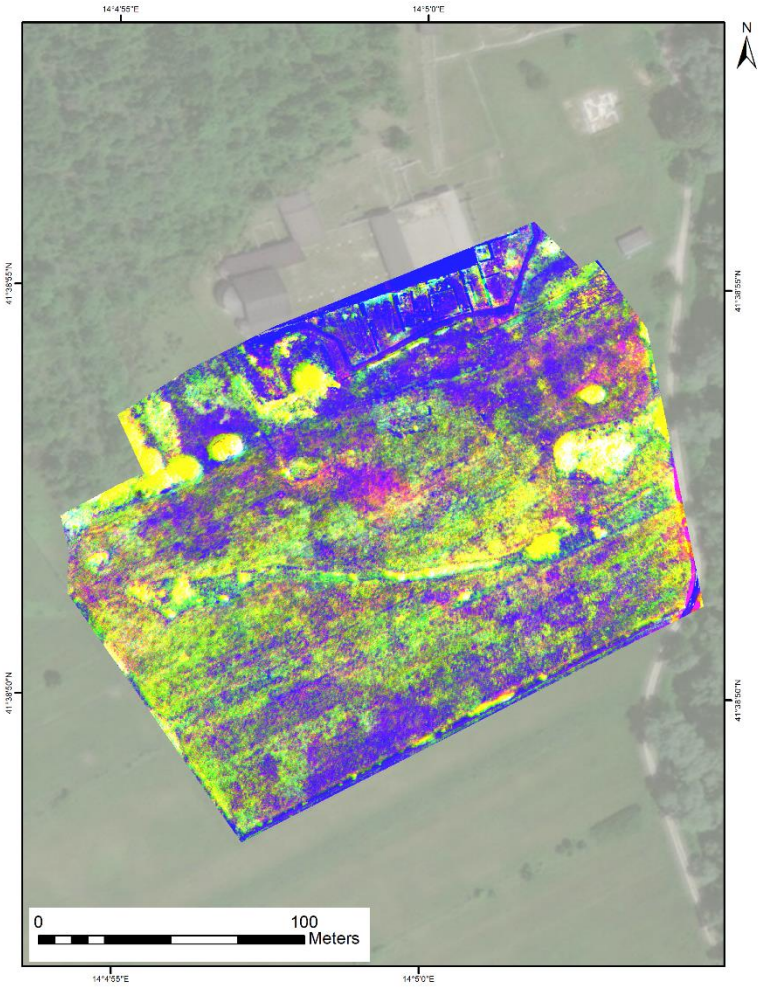

Figure 12. SPCAs obtained using correlation-matrix method. R: 4th PC; G: 23rd PC; B: 27th PC.

Useful PCs were considered in RGB combination, as previously used in the field of RS for CH, since analysing all of them would not have benefited the analysis and would have frustrated the SPCA data-reduction process [92,93].

3. Results

The analysis was carried out on all the images produced (single images, indices and transformed images) for the identification of single features, trying to match archaeological ancillary data with the multispectral one. The creation of indices (spectral enhancement) was undoubtedly a mandatory step for archaeological research. On the other hand, even SPCA transformation was fundamental, as well as radiometric enhancement, with standard deviation displays at ±1.5–2 σ (Figure 12).

An important step was represented by the autoptical analysis of the images produced, which showed significant differences due to the individual channels involved (see data processing). Single channels (NIR, Red, Green, Red-Edge) over time, showed different features due to the state of growth of the vegetation in the area, influenced by seasons and human action. The visibility of features was also influenced by the radiometric enhancement methodologies applied. An improved result was observed for the combination of the individual bands in RGB images (Red: Nir band; Green: Red band; Blue: Green band) for each acquisition date, using AHE and standard deviation (±2 σ), and in the calculated indices, according to spectral response and M statistic (Figure 13).

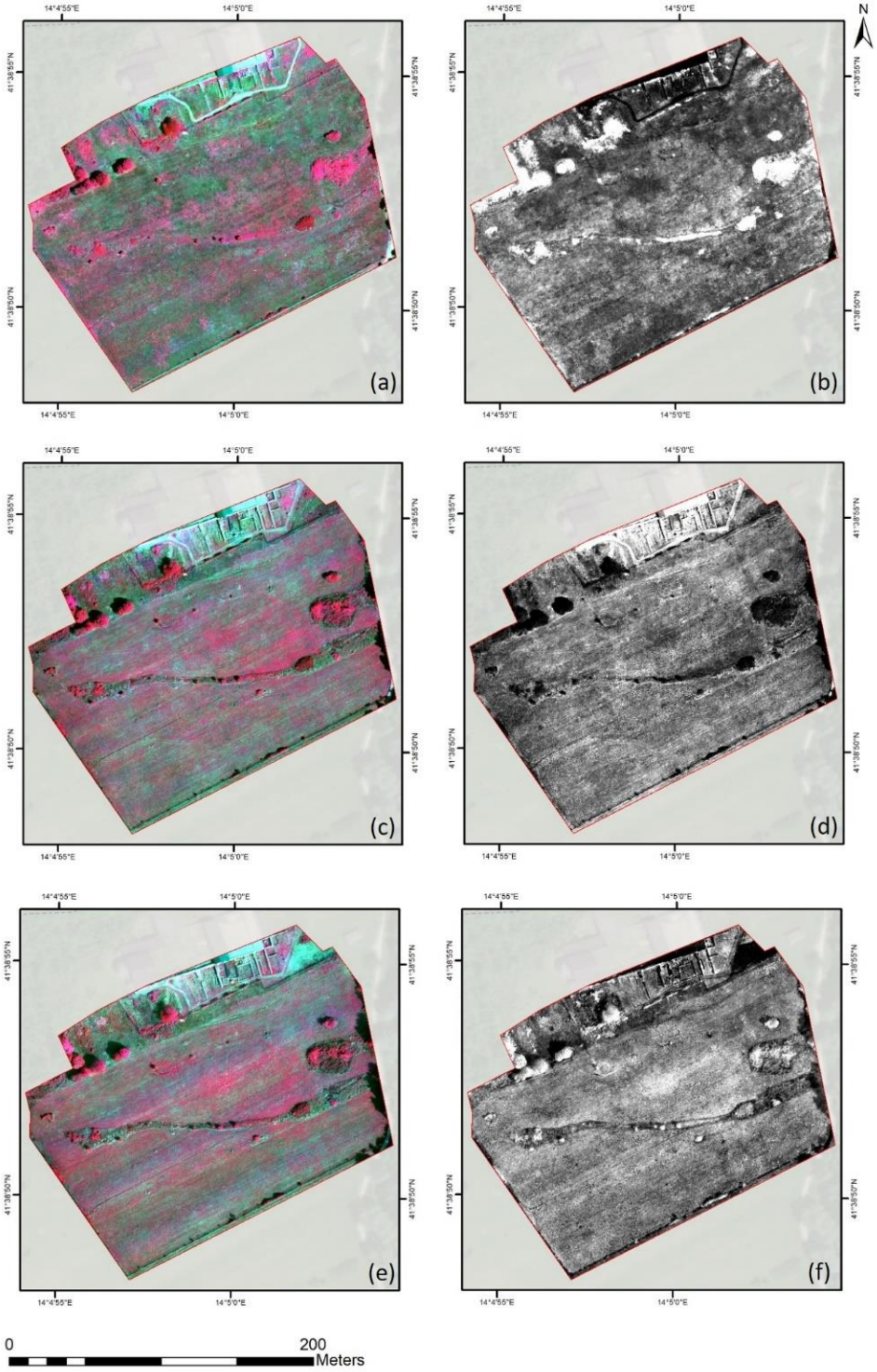

Figure 13. (**a**) July FCIR; (**b**) July NLI with M = 6.4; (**c**) August FCIR; (**d**) August OSAVI with M = 2.6; (**e**) September FCIR; (**f**) September GNDVI with M = 3.1. All views were obtained using radiometric enhance standard deviation (±2 σ) method.

However, the best result was obtained, as expected, by the SPCA, enhanced using radiometric enhancement methodologies, which provided in a single RGB composition, with selected principal components (PCs), most of the useful information observed within the individual bands and the different indices. The SPCA obtained from the correlation matrix and combined in RGB using 4th, 23rd, 27th PCs, was considered to be the most suitable for the visualisation of features of archaeological interest (Figure 12).

4. Discussion

Archaeological indicators, as well as other features, were well identifiable within the individual images produced. Furthermore, the high resolution of the acquisitions allowed the easy identification of different types of features [94] such as (i) possible buried structures; (ii) changes in the permeability and depth of the soil; (iii) traces of agricultural vehicles; (iv) traces of canals and channels or paths; (v) recent traces of vehicles. The identified features in the acquired data were analysed trying to separate the evidence of archaeological interest from those of no archaeological interest, using simultaneously data from RS and ancillary data (literature, excavation reports, etc.). In particular, in order to avoid data redundancy and maximise the information, the RGB combination produced from the SPCA shown in the Figure 12 was used as the reference image, as it was considered to be the best compromise produced during the study phase. The SPCA operation was fundamental in reducing the useless input information, thresholding the useful images by spectral statistics ($M > 1$) and concentrating through PCA only the bands considered to be performing for the archaeological study.

4.1. Non-Archaeological Features

The most evident features were certainly those left by the agricultural vehicles that pass through the field. The field, in fact, although no longer subject to agricultural activity, has been used in the past for crops, olive groves, orchards, and vineyard as the entire area around the abbey of San Vincenzo al Volturno [95]. Moreover, still today it is crossed by vehicles and people to reach the inner fields, and vegetation is cut regularly. These features were easy to identify for several reasons: (i) are regular, composed by two parallel lines running at a distance of 170/200 cm from each other; (ii) in most cases, are east–west oriented, from the river to the hinterland; (iii) have a low value in canopies-health indices and bands. Agricultural traces have been identified within the whole field, from a macroscopic point of view, as deep linear signs SW–NE oriented, according to IGM images (Figure 3). These are certainly the result of a previous agricultural vocation of the area, but, probably, are also dictated by the natural course of the soil deposits near the embankment of the river Volturno. Other anthropic signs were identified in those left by the cultivation of the tree, and traces left by rearrangement activities in the area following archaeological excavation or field stripping. The traces seem to be directed towards a vegetated area, where vegetation has grown over a large amount of stones and lithic elements, probably piled up (Figure 14).

4.2. Features of Archaeological Interest (FoAI)

Features with regular geometric shape were identified in multispectral images, indices, and PCs. The identification was carried out using archaeological hypothesis made in the past on the development of the abbey. According to these considerations, the monastery developed in a southerly direction, with a cloister, after the 9th century, assuming a scheme that could be considered similar to that depicted on the well-known Plan of St. Gall, or other monasteries of the late Middle Ages [96,97].

Most of the FoAI identified within the survey area fall in the area immediately outside the fence of the archaeological site, enclosed between the Basilica Maior and a landscape-barrier consisting of trees and vegetation (probably the remains of a border wall or a canal). The FoAI are clearly visible, above all, in SPCA. FoAI have showed an extremely complex pattern. The main problem is represented by the overlapping of structures and events during the different phases of the life of the abbey, which is present in the area as it is visible within the excavated areas. The features have been divided into two macro-groups based on the angle with respect to the West–East axis, to be studied from a macroscopic point of view in the whole context: (i) FoAI with an angle of 10/25 degrees and their orthogonals; (ii) FoAI with an angle of 25/45 degrees and their orthogonals (Figure 15).

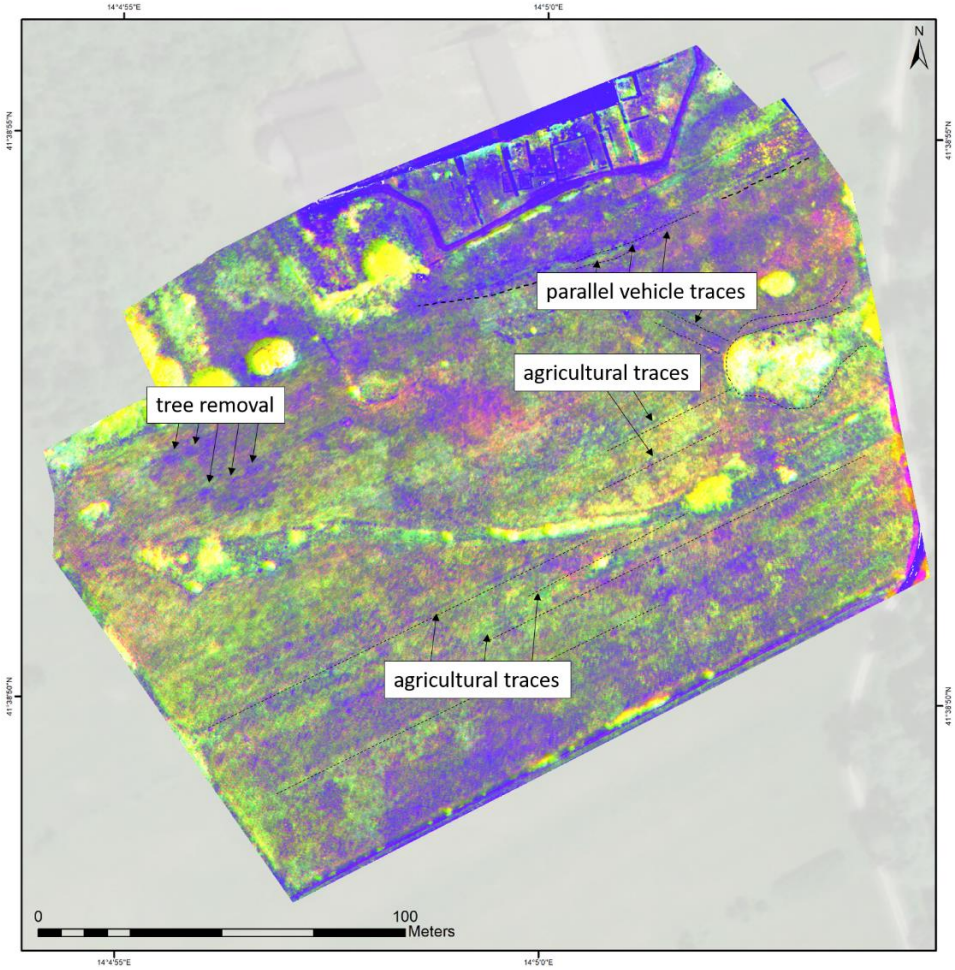

Figure 14. SPCA with annotation of features of no archaeological interest. Examples of vehicle traces, agricultural traces and traces left by the removal of trees are outlined and indicated by arrows.

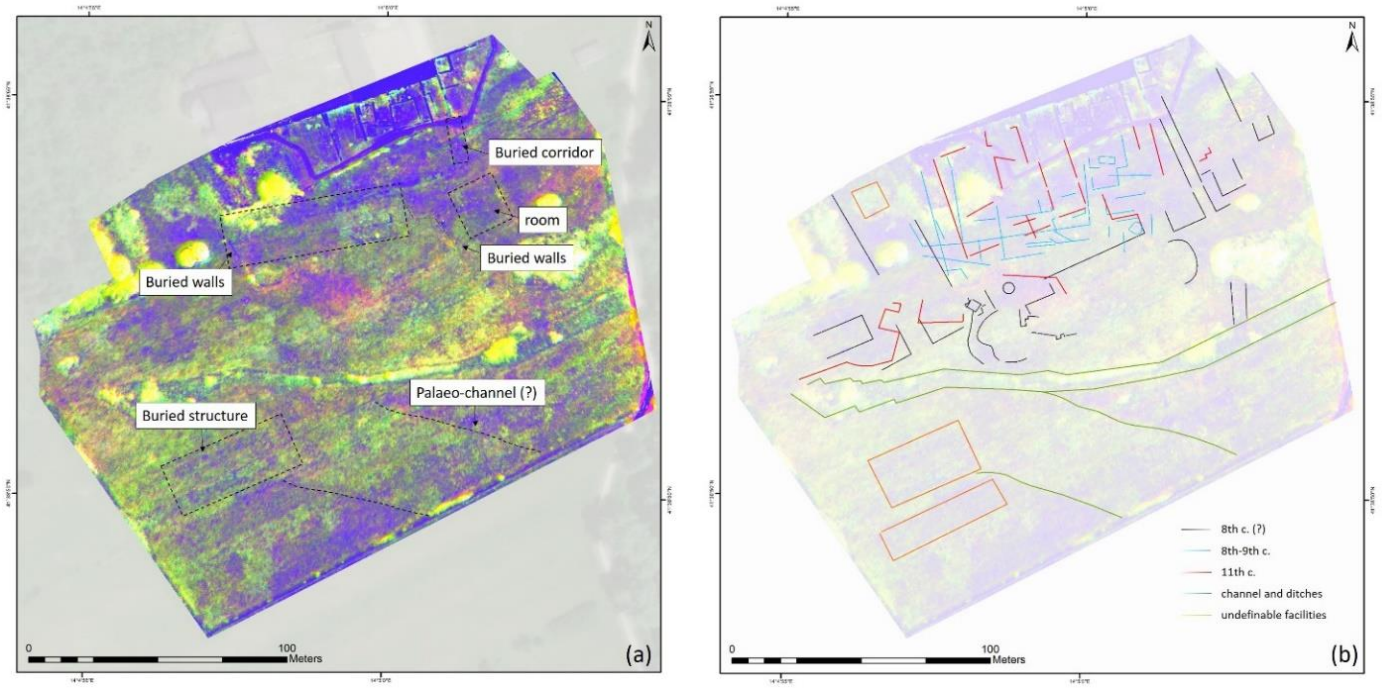

Figure 15. SPCA and identified features and hypothesis: (**a**) example of FoAIs; (**b**) identified FoAIs.

The first appreciable group of features is located immediately south of the Basilica, and suggests probably, an extension south of the monastic workshop. This evidence probably belongs to the 2nd architectural phase of the monastic settlement (9th century). The second group of structures is characterised by the extension of two parallel walls which create an extension of the corridor between "atrium" and the structures of monumental upstairs to the basilica. The East wall probably turns left, where we can observe a NW–SE wall. This evidence could belong to the 5th building phase, as the wall which starts from the room on the south side of the apses. This structure turns left and creates with pre previous walls a kind of corridor (with "C" plan). Actually, it is hard to understand if these structures belong to the same building activities in which appear also the walls of the "cloister" (11th century) (Figure 16).

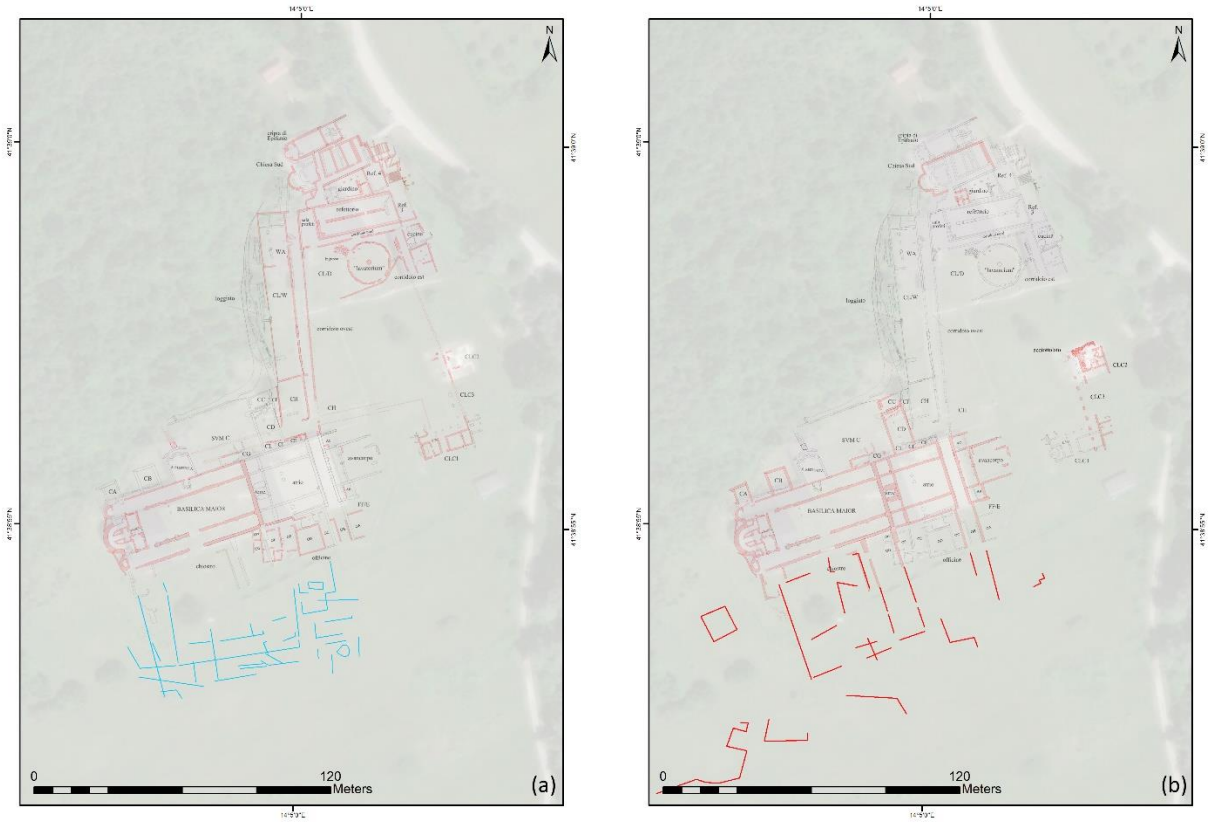

Figure 16. Identified features: (**a**) 2nd phase (9th century); (**b**) 5th phase (11th century).

However, the main doubt is represented by another group of features. On the East side of the plan: two parallel walls with North–South orientation which arrive near another group of structures that seems to describe a large building with two apses on the East side. Whereas, the features on the West side of this buildings are probably the traces of collapsed walls. The building with apses is parallel to a long wall (with SW/NE orientation) that could represent part of the monastic defensive wall on its South side, although there are other buildings south of it. Finally, we can notice how the hypothetical defensive wall crosses the water ditch that could belong to a roman or pre-roman phase, according to the other ditches visible in the plane of Rocchetta, around the new Abbey [98].

5. Conclusions

The use of multispectral images over time, of the same area, has allowed to identify elements whose visibility is closely linked to phenology, confirming what is already known in literature on the issue [31,38,70–72]. According to what has been observed in the images, indices and graphs reported, the visibility of the archaeological proxy indicators has been

influenced by anthropic and climatic factors, which have modified the phenology and the state of the vegetation. This phenomenon made all the images acquired useful, although the July image seems to differ from the August and September images, which are quite similar. In the data acquired in August and September, vegetation was influenced by a cut-operation, which took place at the beginning of August, and has showed signs of regrowth strongly influenced by the presence of buried elements, differences in soil permeability, as well as traces left by the vehicles. The phenology has allowed to obtain more evidence of small features in sharp contrast to the background. On the contrary, the data acquired in July showed a widespread growth of vegetation whose health was reflected in the strong zonal spectral differences recorded within the several bands and enhanced by the creation of FCIRs and indices. This has allowed the identification of linear 'macro-features' probably created by the presence of extensive elements in the subsoil that impact on soil characteristics and the natural development of vegetation. PCAs played a crucial role in the trade-off between avoiding the loss of useful information and reducing the number of images to be considered, due to the differences between the acquisitions. The use of selective PCA (SPCA), already employed in the past in other studies, was fundamental in this case, but allowed considerations to be made on acquisitions at a larger scale, making the entire process replicable and scalable. In fact, the methodology of identifying the features of archaeological interest, for the reconstruction of the ancient monastery, was facilitated by the use of statistics (M statistic) and the SPCA transformation, reducing the number of source images to be analysed to a single RGB composition. Of course, this represented a compromise, however, in view of a general methodology, applicable to optical big- and multitemporal-data (e.g., multispectral and hyperspectral), the data-reduction is a mandatory step and SPCA could be a good choice.

RS and UAS technologies have been useful for the discovery phase of the archaeological site of San Vincenzo al Volturno. Acquisitions have allowed to cover a large area, impossible to investigate with the techniques of archaeological excavation. However, the contribution of knowledge provided by previous archaeological investigations, published material, and the experience of those who have worked on the site for years has been of fundamental importance for the connotation of the results acquired by the RS techniques. Analyses have increased our knowledge of one of the most important religious and economic sites in medieval Europe and have partly changed the idea of the planimetric development of the monastery, as supposed in Figure 2 and literature. At the same time, these totally non-invasive activities allowed to consider new proposals for the investigation, protection and preservation of the buried structures outside the current boundary of the archaeological site.

Author Contributions: Conceptualisation, N.A., A.F., F.M. and R.L.; methodology, N.A.; software, N.A.; validation, A.F., F.M. and R.L.; formal analysis, N.A. and A.F.; investigation, N.A. and A.F.; resources, N.M. and R.L.; data curation, N.A.; writing—original draft preparation, N.A.; writing—review and editing, F.M., N.M. and R.L.; supervision, F.M., N.M. and R.L.; project administration, R.L. All authors have read and agreed to the published version of the manuscript.

Funding: This research received no external funding.

Institutional Review Board Statement: Not applicable.

Informed Consent Statement: Not applicable.

Acknowledgments: Special thanks to the Soprintendenza Archeologia, Belle Arti E Paesaggio del Molise and the Polo Museale del Molise for having granted the necessary permits to fly and acquire data.

Conflicts of Interest: The authors declare no conflict of interest.

References

1. Bewley, R.H. Aerial survey for archaeology. *Photogramm. Rec.* **2003**, *18*, 273–292. [CrossRef]
2. Campana, S. Drones in Archaeology. State-of-the-art and Future Perspectives. *Archaeol. Prospect.* **2017**, *24*, 275–296. [CrossRef]

3. Gojda, M. The Contribution of Aerial Archaeology to European Landscape Studies: Past Achievements, Recent Developments and Future Perspectives. *J. Eur. Archaeol.* **1997**, *5*, 91–104. [CrossRef]
4. Corsi, C.; Slapšak, B.; Vermeulen, F. (Eds.) *Good Practice in Archaeological Diagnostics: Non-Invasive Survey of Complex Archaeological Sites*, 1st ed.; Natural Science in Archaeology; Springer International Publishing: Cham, Switzerland, 2013; ISBN 978-3-319-01784-6.
5. Adamopoulos, E.; Rinaudo, F. UAS-Based Archaeological Remote Sensing: Review, Meta-Analysis and State-of-the-Art. *Drones* **2020**, *4*, 46. [CrossRef]
6. Chiabrando, F.; D'Andria, F.; Sammartano, G.; Spanò, A. UAV photogrammetry for archaeological site survey. 3D models at the Hierapolis in Phrygia (Turkey). *Virtual Archaeol. Rev.* **2018**, *9*, 28. [CrossRef]
7. Cowley, D.C.; Moriarty, C.; Geddes, G.; Brown, G.L.; Wade, T.; Nichol, C.J. UAVs in Context: Archaeological Airborne Recording in a National Body of Survey and Record. *Drones* **2017**, *2*, 2. [CrossRef]
8. Everaerts, J. The Use of Unmanned Aerial Vehicles (UAVs) for Remote Sensing and Mapping. *Int. Arch. Photogramm. Remote Sens. Spat. Inf. Sci.* **2008**, *37*, 1187–1192.
9. Gasparini, M.; Moreno-Escribano, J.C.; Monterroso-Checa, A. Photogrammetric Acquisitions in Diverse Archaeological Contexts Using Drones: Background of the Ager Mellariensis Project (North of Córdoba-Spain). *Drones* **2020**, *4*, 47. [CrossRef]
10. Luis-Ruiz, J.; Sedano-Cibrián, J.; Pereda-García, R.; Pérez-Álvarez, R.; Malagón-Picón, B. Optimization of Photogrammetric Flights with UAVs for the Metric Virtualization of Archaeological Sites. Application to Juliobriga (Cantabria, Spain). *Appl. Sci.* **2021**, *11*, 1204. [CrossRef]
11. Megarry, W.; Graham, C.; Gilhooly, B.; O'Neill, B.; Sands, R.; Nyland, A.; Cooney, G. Debitage and Drones: Classifying and Characterising Neolithic Stone Tool Production in the Shetland Islands Using High Resolution Unmanned Aerial Vehicle Imagery. *Drones* **2018**, *2*, 12. [CrossRef]
12. Sammartano, G.; Chiabrando, F.; Spanò, A. Oblique Images and Direct Photogrammetry with a Fixed Wing Platform: First Test and Results in Hierapolis of Phrygia (Tk). *Int. Arch. Photogramm. Remote Sens. Spat. Inf. Sci.* **2020**, *43*, 75–82. [CrossRef]
13. Rinaudo, F.; Chiabrando, F.; Lingua, A.; Spanò, A. Archaeological Site Monitoring: Uav Photogrammetry can be an Answer. *Int. Arch. Photogramm. Remote Sens. Spat. Inf. Sci.* **2012**, *39*, 583–588. [CrossRef]
14. Agudo, P.U.; Pajas, J.A.; Pérez-Cabello, F.; Redón, J.V.; Lebrón, B.E. The Potential of Drones and Sensors to Enhance Detection of Archaeological Cropmarks: A Comparative Study Between Multi-Spectral and Thermal Imagery. *Drones* **2018**, *2*, 29. [CrossRef]
15. Aqdus, S.A.; Hanson, W.S.; Drummond, J. The potential of hyperspectral and multi-spectral imagery to enhance archaeological cropmark detection: A comparative study. *J. Archaeol. Sci.* **2012**, *39*, 1915–1924. [CrossRef]
16. Brooke, C.; Clutterbuck, B. Mapping Heterogeneous Buried Archaeological Features Using Multisensor Data from Unmanned Aerial Vehicles. *Remote Sens.* **2019**, *12*, 41. [CrossRef]
17. Casana, J.; Wiewel, A.; Cool, A.; Hill, A.C.; Fisher, K.D.; Laugier, E. Archaeological Aerial Thermography in Theory and Practice. *Adv. Archaeol. Pr.* **2017**, *5*, 310–327. [CrossRef]
18. Cavalli, R.M.; Colosi, F.; Palombo, A.; Pignatti, S.; Poscolieri, M. Remote hyperspectral imagery as a support to archaeological prospection. *J. Cult. Herit.* **2007**, *8*, 272–283. [CrossRef]
19. Hill, A.C.; Laugier, E.J.; Casana, J. Archaeological Remote Sensing Using Multi-Temporal, Drone-Acquired Thermal and Near Infrared (NIR) Imagery: A Case Study at the Enfield Shaker Village, New Hampshire. *Remote Sens.* **2020**, *12*, 690. [CrossRef]
20. James, K.; Nichol, C.J.; Wade, T.; Cowley, D.; Poole, S.G.; Gray, A.; Gillespie, J. Thermal and Multispectral Remote Sensing for the Detection and Analysis of Archaeologically Induced Crop Stress at a UK Site. *Drones* **2020**, *4*, 61. [CrossRef]
21. Šedina, J.; Housarová, E.; Raeva, P. Using RPAS for the detection of archaeological objects using multispectral and thermal imaging. *Eur. J. Remote Sens.* **2018**, *52*, 182–191. [CrossRef]
22. Corns, A.; Shaw, R. High resolution 3-dimensional documentation of archaeological monuments & landscapes using airborne LiDAR. *J. Cult. Herit.* **2009**, *10*, e72–e77. [CrossRef]
23. Davis, D.S.; Sanger, M.C.; Lipo, C.P. Automated mound detection using lidar and object-based image analysis in Beaufort County, South Carolina. *Southeast. Archaeol.* **2019**, *38*, 23–37. [CrossRef]
24. Masini, N.; Coluzzi, R.; Lasaponar, R. On the Airborne Lidar Contribution in Archaeology: From Site Identification to Landscape Investigation. In *Laser Scanning, Theory and Applications*; Wang, C.-C., Ed.; InTech: Princeton, NJ, USA, 2011; ISBN 978-953-307-205-0.
25. Ronchi, D.; Limongiello, M.; Barba, S. Correlation among Earthwork and Cropmark Anomalies within Archaeological Landscape Investigation by Using LiDAR and Multispectral Technologies from UAV. *Drones* **2020**, *4*, 72. [CrossRef]
26. Stott, D.; Boyd, D.S.; Beck, A.; Cohn, A.G. Airborne LiDAR for the Detection of Archaeological Vegetation Marks Using Biomass as a Proxy. *Remote Sens.* **2015**, *7*, 1594–1618. [CrossRef]
27. De Reu, J.; Plets, G.; Verhoeven, G.; De Smedt, P.; Bats, M.; Cherretté, B.; De Maeyer, W.; Deconynck, J.; Herremans, D.; Laloo, P.; et al. Towards a three-dimensional cost-effective registration of the archaeological heritage. *J. Archaeol. Sci.* **2013**, *40*, 1108–1121. [CrossRef]
28. Nex, F.; Remondino, F. UAV for 3D mapping applications: A review. *Appl. Geomat.* **2014**, *6*, 1–15. [CrossRef]
29. Remondino, F.; Barazzetti, L.; Nex, F.; Scaioni, M.; Sarazzi, D. Uav Photogrammetry for Mapping and 3d Modeling—Current Status and Future Perspectives. *Int. Arch. Photogramm. Remote Sens. Spat. Inf. Sci.* **2011**, 25–31. [CrossRef]

30. Verhoeven, G. Taking computer vision aloft—Archaeological three-dimensional reconstructions from aerial photographs with photoscan. *Archaeol. Prospect.* **2011**, *18*, 67–73. [CrossRef]
31. De Guio, A. Cropping for a Better Future, Vegetation Indices in Archaeology. In *Detecting and Understanding Historic Landscapes*; PCA Studies; SAP: Mantova, Italy, 2015; pp. 23–60. ISBN 978-88-87115-99-4.
32. Tan, K.; Wan, Y.; Zhou, X.; Song, D.; Duan, Q. The application of remote sensing technology in the archaeological study of the Mausoleum of Emperor Qinshihuang. *Int. J. Remote Sens.* **2006**, *27*, 3347–3363. [CrossRef]
33. Wilson, D.R. *Air Photo Interpretation for Archaeologists*, 2nd ed.; The History Press Ltd.: Gloucestershire, UK, 2000.
34. Beck, A. *Archaeological Site Detection: The Importance of Contrast*; ISPRS: Hannover, Germany, 2007; pp. 307–312.
35. Evans, D.; Traviglia, A. Uncovering Angkor: Integrated Remote Sensing Applications in the Archaeology of Early Cambodia. In *Satellite Remote Sensing*; Lasaponara, R., Masini, N., Eds.; Remote Sensing and Digital Image Processing; Springer: Dordrecht, The Netherlands, 2012; Volume 16, pp. 197–230. ISBN 978-90-481-8800-0.
36. Kaimaris, D.; Patias, P.; Tsakiri, M. Best period for high spatial resolution satellite images for the detection of marks of buried structures. *Egypt. J. Remote Sens. Space Sci.* **2012**, *15*, 9–18. [CrossRef]
37. Kalayci, T.; Lasaponara, R.; Wainwright, J.; Masini, N. Multispectral Contrast of Archaeological Features: A Quantitative Evaluation. *Remote Sens.* **2019**, *11*, 913. [CrossRef]
38. Lasaponara, R.; Masini, N. (Eds.) *Satellite Remote Sensing: A New Tool for Archaeology*; Remote Sensing and Digital Image Processing; Springer: Dordrecht, The Netherlands; New York, NY, USA, 2012; ISBN 978-90-481-8800-0.
39. Masini, N.; Marzo, C.; Manzari, P.; Belmonte, A.; Sabia, C.; Lasaponara, R. On the characterization of temporal and spatial patterns of archaeological crop-marks. *J. Cult. Herit.* **2018**, *32*, 124–132. [CrossRef]
40. Cowley, D. *Remote Sensing for Archaeology and Heritage Management—Site Discovery, Interpretation and Registration*; Academia: San Francisco, CA, USA, 2011; pp. 43–55. ISBN 978-963-9911-20-8.
41. Lillesand, T.; Kiefer, R.W.; Chipman, J. *Remote Sensing and Image Interpretation*, 6th ed.; John Wiley and Sons: Hoboken, NJ, USA, 2018.
42. Agapiou, A.; Lysandrou, V.; Hadjimitsis, D.G. Optical Remote Sensing Potentials for Looting Detection. *Geosciences* **2017**, *7*, 98. [CrossRef]
43. Agapiou, A.; Hadjimitsis, D.G.; Alexakis, D.D. Evaluation of Broadband and Narrowband Vegetation Indices for the Identification of Archaeological Crop Marks. *Remote Sens.* **2012**, *4*, 3892–3919. [CrossRef]
44. Bennett, R.; Welham, K.; Hill, R.A.; Ford, A.L.J. The Application of Vegetation Indices for the Prospection of Archaeological Features in Grass-dominated Environments. *Archaeol. Prospect.* **2012**, *19*, 209–218. [CrossRef]
45. Calleja, J.F.; Pagés, O.R.; Díaz-Álvarez, N.; Peón, J.; Gutiérrez, N.; Martín-Hernández, E.; Relea, A.C.; Melendi, D.R.; Álvarez, P.F. Detection of buried archaeological remains with the combined use of satellite multispectral data and UAV data. *Int. J. Appl. Earth Obs. Geoinf.* **2018**, *73*, 555–573. [CrossRef]
46. Hodges, R.; Mitchell, J. (Eds.) *San Vincenzo al Volturno: The Archaeology, Art, and Territory of an Early Medieval Monastery*; BAR International Series; B.A.R.: Oxford, UK, 1985; ISBN 978-0-86054-323-7.
47. Marazzi, F. San Vincenzo al Volturno Nel Passaggio All'età Normanna (Secoli XI–XII): Riposizionamento Politico e Ristrutturazione Materiale. In *Il Molise dai Normanni Agli Aragonesi: Arte e Archeologia*; Torrossa: Fiesole, Italy, 2012.
48. Marazzi, F. (Ed.) *La "Basilica Maior" Di San Vincenzo al Volturno (Scavi 2000–2007)*; Studi Vulturnensi, Volturnia edizioni; IRIS: Cerro al Volturno, Italy, 2014; ISBN 978-88-96092-23-1.
49. Leppard, S.; Hodges, R.A.; Mitchell, J. *San Vincenzo 5—Excavations of San Vincenzo Maggiore and the Associated Temporary and Collective Workshops*; Archaeology Data Service: York, UK, 2009.
50. Marazzi, F. *Archeologia Della Parola: Percorsi e Strumenti per la Tradizione Della Memoria nel MONASTERO di San Vincenzo al Volturno*; IRIS: Cerro al Volturno, Italy, 2012; ISBN 978-88-96092-14-9.
51. Banerjee, R.; Srivastava, P.K. Reconstruction of contested landscape: Detecting land cover transformation hosting cultural heritage sites from Central India using remote sensing. *Land Use Policy* **2013**, *34*, 193–203. [CrossRef]
52. Bradford, J.S.P. The Apulia Expedition: An Interim Report. *Antiquity* **1950**, *24*, 84–94. [CrossRef]
53. Bradford, J. 'Buried Landscapes' in Southern Italy. *Antiquity* **1949**, *23*, 58–72. [CrossRef]
54. Furlanetto, P.; Bondesan, A. Geomorphological evolution of the plain between the Livenza and Piave Rivers in the sixteenth and seventeenth centuries inferred by historical maps analysis (Mainland of Venice, Northeastern Italy). *J. Maps* **2014**, *11*, 261–266. [CrossRef]
55. Nicu, I.C.; Stoleriu, C.C. Land use changes and dynamics over the last century around churches of Moldavia, Bukovina, Northern Romania—Challenges and future perspectives. *Habitat Int.* **2019**, *88*, 101979. [CrossRef]
56. Riley, D.N. New aerial reconnaissance in Apulia. *Pap. Br. Sch. Rome* **1992**, *60*, 291–307. [CrossRef]
57. San-Antonio-Gómez, C.; Velilla, C.; Manzano-Agugliaro, F. Urban and landscape changes through historical maps: The Real Sitio of Aranjuez (1775–2005), a case study. *Comput. Environ. Urban Syst.* **2014**, *44*, 47–58. [CrossRef]
58. Schuppert, C.; Dix, A. Reconstructing Former Features of the Cultural Landscape Near Early Celtic Princely Seats in Southern Germany. *Soc. Sci. Comput. Rev.* **2009**, *27*, 420–436. [CrossRef]
59. Weber, S.A.; Yool, S.R. Detection of subsurface archaeological architecture by computer assisted airphoto interpretation. *Geoarchaeology* **1999**, *14*, 481–493. [CrossRef]

60. Theiler, J.P.; Cai, D.M. Resampling Approach for Anomaly Detection in Multispectral Images. In Proceedings of the AeroSense 2003, Orlando, FL, USA, 21–25 April 2003; Volume 5093, pp. 230–241.
61. Conrad, O.; Bechtel, B.; Bock, M.; Dietrich, H.; Fischer, E.; Gerlitz, L.; Wehberg, J.; Wichmann, V.; Böhner, J. System for Automated Geoscientific Analyses (SAGA) v. 2.1.4. *Geosci. Model Dev.* **2015**, *8*, 1991–2007. [CrossRef]
62. Agapiou, A.; Hadjimitsis, D.; Sarris, A.; Georgopoulos, A.; Alexakis, D.D. Optimum temporal and spectral window for monitoring crop marks over archaeological remains in the Mediterranean region. *J. Archaeol. Sci.* **2013**, *40*, 1479–1492. [CrossRef]
63. Lasaponara, R.; Masini, N. On the potential of QuickBird data for archaeological prospection. *Int. J. Remote Sens.* **2006**, *27*, 3607–3614. [CrossRef]
64. Lasaponara, R.; Masini, N. Identification of archaeological buried remains based on the normalized difference vegetation index (NDVI) from Quickbird satellite data. *IEEE Geosci. Remote Sens. Lett.* **2006**, *3*, 325–328. [CrossRef]
65. Campana, S.; Forte, M.; Consiglio Nazionale Delle Ricerche (Italy) (Eds.) *From Space to Place: 2nd International Conference on Remote Sensing in Archaeology, Proceedings of the 2nd International Workshop, CNR, Rome, Italy, 4–7 December 2006*; BAR International Series; Archeopress: Oxford, UK, 2006; ISBN 978-1-84171-998-6.
66. Hum, Y.C.; Lai, K.W.; Salim, M.I.M. Multiobjectives bihistogram equalization for image contrast enhancement. *Complexity* **2014**, *20*, 22–36. [CrossRef]
67. Jensen, J.R. *Introductory Digital Image Processing: A Remote Sensing Perspective*; Pearson Series in Geographic Information Science; Pearson Education, Inc.: Glenview, IL, USA, 2016; ISBN 978-0-13-405816-0.
68. Shanmugavadivu, P.; Balasubramanian, K. Image Inversion and Bi Level Histogram Equalization for Contrast Enhancement. *Int. J. Comput. Appl.* **2010**, *1*, 69–73. [CrossRef]
69. Zimmerman, J.; Pizer, S.; Staab, E.; Perry, J.; McCartney, W.; Brenton, B. An evaluation of the effectiveness of adaptive histogram equalization for contrast enhancement. *IEEE Trans. Med. Imaging* **1988**, *7*, 304–312. [CrossRef]
70. Agapiou, A.; Hadjimitsis, D.G.; Themistocleous, K.; Papadavid, G.; Toulios, L. Detection of archaeological crop marks in Cyprus using vegetation indices from Landsat TM/ETM+ satellite images and field spectroscopy measurements. *Remote Sens.* **2010**, *7831*, 78310. [CrossRef]
71. Sripada, R.P.; Schmidt, J.P.; Dellinger, A.E.; Beegle, D.B. Evaluating Multiple Indices from a Canopy Reflectance Sensor to Estimate Corn N Requirements. *Agron. J.* **2008**, *100*, 1553–1561. [CrossRef]
72. Moriarty, C.; Cowley, D.C.; Wade, T.; Nichol, C.J. Deploying multispectral remote sensing for multi-temporal analysis of archaeological crop stress at Ravenshall, Fife, Scotland. *Archaeol. Prospect.* **2018**, *26*, 33–46. [CrossRef]
73. Gitelson, A.A.; Merzlyak, M.N. Remote sensing of chlorophyll concentration in higher plant leaves. *Adv. Space Res.* **1998**, *22*, 689–692. [CrossRef]
74. Rouse, J.; Haas, R.H.; Deering, D.; Schell, J.A.; Harlan, J. *Monitoring the Vernal Advancement and Retrogradation (Green Wave Effect) of Natural Vegetation. [Great Plains Corridor]*; NASA: Washington, DC, USA, 1973.
75. Huete, A.; Didan, K.; Miura, T.; Rodriguez, E.P.; Gao, X.; Ferreira, L.G. Overview of the radiometric and biophysical performance of the MODIS vegetation indices. *Remote Sens. Environ.* **2002**, *83*, 195–213. [CrossRef]
76. Rowlands, A.; Sarris, A. Detection of exposed and subsurface archaeological remains using multi-sensor remote sensing. *J. Archaeol. Sci.* **2007**, *34*, 795–803. [CrossRef]
77. Huete, A.R.; Liu, H.Q.; Batchily, K.; van Leeuwen, W. A comparison of vegetation indices over a global set of TM images for EOS-MODIS. *Remote Sens. Environ.* **1997**, *59*, 440–451. [CrossRef]
78. Kaufman, Y.; Remer, L. Detection of forests using mid-IR reflectance: An application for aerosol studies. *IEEE Trans. Geosci. Remote Sens.* **1994**, *32*, 672–683. [CrossRef]
79. Luo, L.; Bachagha, N.; Yao, Y.; Liu, C.; Shi, P.; Zhu, L.; Shao, J.; Wang, X. Identifying Linear Traces of the Han Dynasty Great Wall in Dunhuang Using Gaofen-1 Satellite Remote Sensing Imagery and the Hough Transform. *Remote Sens.* **2019**, *11*, 2711. [CrossRef]
80. Hotelling, H. Analysis of a complex of statistical variables into principal components. *J. Educ. Psychol.* **1933**, *24*, 417–441. [CrossRef]
81. Chuvieco, E. *Fundamentals of Satellite Remote Sensing: An Environmental Approach*, 2nd ed.; Taylor & Francis Group: Boca Raton, FL, USA, 2016.
82. Estornell, J.; Martí-Gavliá, J.M.; Sebastiá, M.T.; Mengual, J. Principal component analysis applied to remote sensing. *Model. Sci. Educ. Learn.* **2013**, *6*, 83–89. [CrossRef]
83. Lasaponara, R.; Abate, N.; Masini, N. On the Use of Google Earth Engine and Sentinel Data to Detect Lost Sections of Ancient Roads. The Case of Via Appia. *IEEE Geosci. Remote Sens. Lett.* **2021**, 1–5. [CrossRef]
84. Lasaponara, R.; Masini, N.; Rizzo, E.; Orefici, G. New discoveries in the Piramide Naranjada in Cahuachi (Peru) using satellite, Ground Probing Radar and magnetic investigations. *J. Archaeol. Sci.* **2011**, *38*, 2031–2039. [CrossRef]
85. Agapiou, A. Enhancement of Archaeological Proxies at Non-Homogenous Environments in Remotely Sensed Imagery. *Sustainability* **2019**, *11*, 3339. [CrossRef]
86. Orlando, P.; de Villa, B. Remote Sensing Applications in Archaeology. *Archeol. Calc.* **2011**, *22*, 147–168.
87. Abate, N.; Lasaponara, R. Preventive Archaeology Based on Open Remote Sensing Data and Tools: The Cases of Sant'Arsenio (SA) and Foggia (FG), Italy. *Sustainability* **2019**, *11*, 4145. [CrossRef]

88. Lasaponara, R.; Masini, N. Preserving the Past from Space: An Overview of Risk Estimation and Monitoring Tools. In *GIS and Environmental Monitoring*; Springer Science and Business Media LLC: Berlin/Heidelberg, Germany, 2017; Volume 16, pp. 61–88.
89. Jolliffe, I.T.; Cadima, J. Principal component analysis: A review and recent developments. *Philos. Trans. R. Soc. A Math. Phys. Eng. Sci.* **2016**, *374*, 20150202. [CrossRef]
90. Traviglia, A. *Archaeological Usability of Hyperspectral Images: Successes and Failures of Image Processing Techniques*; BAR: Delhi, India, 2006; pp. 123–130.
91. Abate, N.; Elfadaly, A.; Masini, N.; Lasaponara, R. Multitemporal 2016–2018 Sentinel-2 Data Enhancement for Landscape Archaeology: The Case Study of the Foggia Province, Southern Italy. *Remote Sens.* **2020**, *12*, 1309. [CrossRef]
92. DeRoin, J.-P.; Téreygeol, F.; Heckes, J. Evaluation of very high to medium resolution multispectral satellite imagery for geoarchaeology in arid regions—Case study from Jabali, Yemen. *J. Archaeol. Sci.* **2011**, *38*, 101–114. [CrossRef]
93. Traviglia, A.; Cottica, D. Remote sensing applications and archaeological research in the Northern Lagoon of Venice: The case of the lost settlement of Constanciacus. *J. Archaeol. Sci.* **2011**, *38*, 2040–2050. [CrossRef]
94. Lasaponara, R.; Masini, N. Detection of archaeological crop marks by using satellite QuickBird multispectral imagery. *J. Archaeol. Sci.* **2007**, *34*, 214–221. [CrossRef]
95. Hodges, R.; Mitchell, J.; Coutts, C.M.; British School at Rome, Centro italiano di studi sull'alto Medioevo (Eds.) San Vincenzo al Volturno: The 1980–86 Excavations. In *Archaeological Monographs of the British School at Rome*; British School at Rome: London, UK, 1993; ISBN 978-0-904152-24-1.
96. Horn, W.; Born, E.; Jones, C.W.; Dupree, A.H. *The Plan of St. Gall: A Study of the Architecture & Economy of & Life in a Paradigmatic Carolingian Monastery*; California studies in the History of Art; University of California Press: Berkeley, CA, USA, 1979; ISBN 978-0-520-01724-5.
97. Marazzi, F. *Le Città Dei Monaci: Storia Degli Spazi Che Avvicinano a Dio*, 1st ed.; Architettura; Jaca Book: Milan, Italy, 2015; ISBN 978-88-16-41292-7.
98. Bowes, K.D.; Francis, K.; Hodges, R.; British School at Rome (Eds.) Between Text and Territory: Survey and Excavations in the Terra of San Vincenzo al Volturno. In *Archaeological Monographs of the British School at Rome*; British School at Rome: London, UK, 2006; ISBN 978-0-904152-48-7.